ACS Partner Journal

ACCOUNTS of materials research

pubs.acs.org/amrcda

Article

All-Solid-State Lithium Metal Batteries with Sulfide Electrolytes: Understanding Interfacial Ion and Electron Transport

Changhong Wang, Keegan Adair, and Xueliang Sun*

Cite This: *Acc. Mater. Res.* 2022, 3, 21−32

Read Online

ACCESS | Metrics & More | Article Recommendations

CONSPECTUS: With the ever-growing demand for high energy density and high safety of energy storage technologies, all-solid-state lithium metal batteries (ASSLMBs) including all-solid-state lithium ion batteries (ASSLIBs) and all-solid-state lithium−sulfur batteries (ASSLSBs) have received considerable attention in recent years. To realize ASSLMBs, various solid-state electrolytes have been rapidly developed. Among them, sulfide electrolytes (SEs) demonstrate the highest ionic conductivity (>10 mS·cm^{-1}) and the most favorable mechanical properties. However, the commercialization of SE-based ASSLMBs has been stymied by sluggish interfacial ion and electron transport kinetics, which arises from the detrimental interfacial reactions, poor interfacial solid−solid contact, and lithium dendrite growth. To overcome the interfacial challenges, an insightful understanding of the complex interfacial ion and electron transport processes in SE-based ASSLMBs is of the foremost importance. Although most of the previous review papers underscored the interfacial challenges and summarized the corresponding strategies, a fundamental understanding of the interfacial ions and electron-transport kinetics in SE-based ASSLMBs has not yet been presented. This Account therefore primarily summarizes our recent understanding of SE-based ASSLMBs from the perspectives of interfacial ion and electron transport, aiming to provide an insightful understanding of interfacial kinetics.

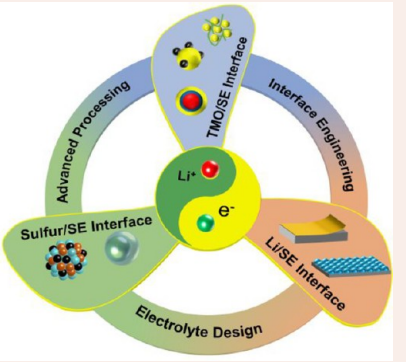

We first compare various solid-state electrolytes including SEs, oxide electrolytes, halide electrolytes, polymer electrolytes, borohydride electrolytes in terms of their ionic conductivity, electrochemical stability windows, and mechanical properties, aiming to justify the advantages of SEs in ASSLMBs. Then, the interfacial challenges at both cathode and anode interfaces of SE-based ASSLIBs and SE-based ASSLSBs are presented, respectively. These interfacial challenges significantly hinder the interfacial ion and electron transport. To boost the interfacial charge transfer kinetics, our recent research advances related to the cathode interface between transition-metal oxides (TMOs) and SEs are then discussed. In parallel, our latest progress on SE-based ASSLSBs is also summarized from the perspective of interfacial kinetics. At the anode interface, our innovative strategies to enhance interfacial Li ion transport between Li metal and SEs are recapped. Finally, conclusions and our perspectives on SE-based ASSLMBs are presented. We believe that this specific Account provides an insightful understanding of interfacial ion and electron transport behavior in SE-based ASSLMBs.

1. INTRODUCTION

Commercial lithium ion batteries (LIBs) have successfully dominated consumer electronics and electric vehicle markets for decades. However, concerns about their safety have become the most prominent issue with the continuous increase in energy density. The serious safety hazards originate from the toxic and flammable organic liquid electrolytes and thermally unstable polymeric separators. In this scenario, developing solid-state electrolytes to replace conventional flammable liquid electrolytes and polymeric separators is the ultimate solution to eradicate the safety issues of LIBs. To this goal, various solid-state electrolytes have been rapidly developed over the past decades, including solid-state oxide electrolytes, solid-state sulfide electrolytes (SEs),[1] solid-state halide electrolytes,[2−7] solid-state polymer electrolytes,[8,9] and solid-state borohydrides.[10,11] Nevertheless, these solid-state electrolytes have their respective advantages and disadvantages. For example, oxide-based solid electrolytes demonstrate wide electrochemical windows and good air stability, but their mechanical stiffness is unfavorable for large-scale roll-to-roll manufacturing. SEs show the highest room-temperature ionic conductivity among these choices, but their moisture sensitivity and narrow electrochemical windows have limited their application. Recently revived halide electrolytes demonstrated high ionic conductivity, high-voltage stability, and favorable mechanical properties; however, their instability against lithium metal anodes has

Received: June 21, 2021
Revised: September 22, 2021
Published: October 19, 2021

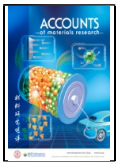

https://doi.org/10.1021/accountsmr.1c00137
Acc. Mater. Res. 2022, 3, 21−32

remained a challenge. Solid-state polymer electrolytes have favorable mechanical properties and wide electrochemical windows, which are the only solid-state electrolyte that has been commercialized so far. However, their low room-temperature (RT) ionic conductivity is unfavorable, particularly for all-climate batteries. Borohydride-based SSEs illustrate a high RT ionic conductivity but narrow electrochemical windows. Moreover, their thermal stability (release of H_2 at a moderate temperature) is a potential risk for practical application. Nevertheless, the narrow electrochemical windows of solid-state borohydrides also limited their application in high-voltage all-solid-state lithium metal batteries (ASSLMBs).

Among those solid-state electrolytes, only SEs displayed the highest room-temperature ionic conductivity (>10 $mS{\cdot}cm^{-1}$), which even overtakes that of conventional liquid electrolytes (approximately 10 $mS{\cdot}cm^{-1}$), thus being regarded as the most promising solid-state electrolytes for developing ASSLMBs. However, SE-based ASSLMBs face significant interface challenges, such as detrimental interfacial reactions, poor solid−solid ionic contact, SE decomposition by carbon additives, polymeric binders blocking ion transport, lithium dendrite growth, drastic volumetric change upon cycling, particularly with high-nickel cathodes, sulfur cathodes, and ultrathin lithium metal anodes. Therefore, addressing interfacial challenges and understanding interfacial charge transfer kinetics is of foremost importance for developing ASSLMBs with both a high energy density and unparalleled safety.

In this Account, we start with the comparison of various solid-state electrolytes, aiming to justify the advantages of SEs in ASSLMBs. Then interfacial challenges of SE-based ASSLIBs are presented in comparison with SE-based ASSLSBs. To overcome these interface challenges, our research advances related to the cathode interface between transition-metal oxides (TMOs) and SEs are summarized from the perspective of interfacial ion and electron transport kinetics. In parallel, our latest progress on understanding interfacial charge transfer in SE-based ASSLSBs is also discussed. Furthermore, the progress and fundamental understanding of the interface between Li metal and SEs are recapped. Finally, conclusions and our perspectives in SE-based ASSLMBs are presented. We believe that this Account willl provide an insightful understanding of SE-based ASSLMBs, particularly from the perspective of the interfacial charge transfer kinetics.

2. COMPARISON OF VARIOUS SOLID-STATE ELECTROLYTES

A solid-state electrolyte is an indispensable component in ASSLMBs, which has been remarkably developed over the past few years. For an ideal solid electrolyte, it should possess a variety of properties, such as low electronic conductivity, high ionic conductivity, a unity transfer number, good mechanical properties, low cost, air stability, and viability for large-scale production. Here, the mainstream solid-state electrolytes are compared from the perspectives of their RT ionic conductivity and electrochemical windows (Figure 1). The representative solid-state oxide electrolytes include garnet-type $Li_7La_3Zr_2O_{12}$ (LLZO), NASICON-type $Li_{1.4}Al_{0.4}Ti_{1.6}(PO_4)_3$ (LATP), perovskite-type $Li_{3x}La_{2/3-x}TiO_3$ (LLTO), and lithium phosphorus oxynitride (LIPON). Among them, most exhibit a high ionic conductivity of over 10^{-4} $S{\cdot}cm^{-1}$, except for LIPON, which has a relatively lower ionic conductivity (10^{-6} $S{\cdot}cm^{-1}$) and is generally used for thin-film batteries. In terms of electrochemical windows, LATP and LAGP are not stable against lithium metal

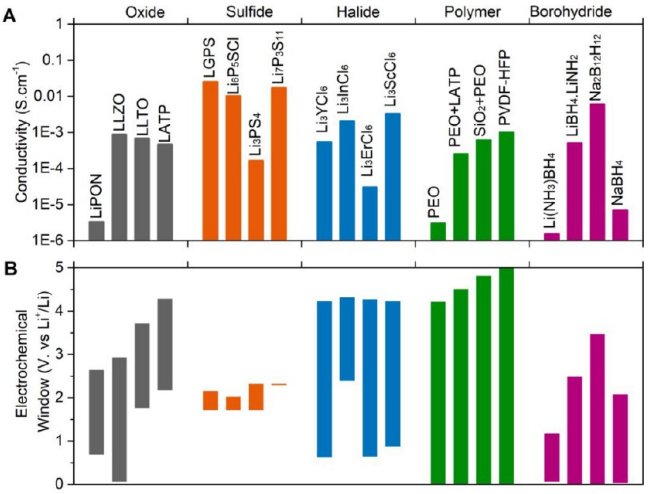

Figure 1. Comparison of room-temperature ionic conductivity (A) and an electrochemical window (B) of various SSEs. The data of stable electrochemical windows was adapted from ref 12−14. Copyrights: 2016, Royal Society of Chemistry; 2019, Wiley-VCH; and 2015, American Chemical Society.

because of the reduction tendency of Ti^{4+} and Ge^{4+}.[15,16] Comparatively, garnet-type LLZO shows better stability against lithium metal and demonstrates much wider electrochemical windows. In addition, oxide electrolytes generally exhibit a high shear modulus, which is assumed to be beneficial for lithium dendrite suppression. However, their high mechanical strength may limit the interfacial ionic contact with electrodes.

Compared with oxygen anions, the sulfur anion is more polarizable, which facilitates fast lithium ion transport. Therefore, the room-temperature ionic conductivity of SEs is much higher than that of oxide electrolytes and the mechanical property is much softer. Some ternary SEs, i.e., $Li_{10}GeP_2S_{12}$ (LGPS)[17] and $Li_{9.54}Si_{1.74}P_{1.44}S_{11.7}Cl_{0.3}$,[18] demonstrate a high ionic conductivity of over 10^{-2} $S{\cdot}cm^{-1}$. However, the main drawback of SEs is their narrow electrochemical windows (Figure 1), which endows significant interfacial reactions with electrode materials. Nevertheless, the high moisture sensitivity of SEs also limited their wide application. Our group has developed air-stable SEs through the doping of soft acids (Sb^{5+}, Sn^{4+}), which demonstrates not only significantly improved air stability but also significantly increased ionic conductivity.[1,19,20] To compensate for the narrow electrochemical windows of SEs, solid-state halide electrolytes with a general formula of A_3MX_6 (A = Li^+, Na^+; M = trivalent metal ions; and X = F−, Cl−, Br−, and I−) have been revisited in recent years because of their high-voltage stability, high room-temperature ionic conductivity, and moderate mechanical property.[2,13] Our group has developed a series of halide electrolytes (Li_3InCl_6,[3,5] $Li_3Y_{1-x}In_xCl_6$,[21] Li_3ScCl_6,[22] Li_3YBr_6,[23] etc.) with high ionic conductivities greater than 10^{-3} $S{\cdot}cm^{-1}$ via both mechanochemical synthesis and liquid-phase synthesis.[3,4,7] Our encouraging achievements in solid-state halide electrolytes have inspired a new wave of research enthusiasm in solid-state halide electrolytes and their application in solid-state batteries.[4,6]

Solid-state borohydride electrolytes have also been developed and have been shown to possess high ionic conductivity of over 10^{-3} $S{\cdot}cm^{-1}$.[11] In addition, solid-state borohydride electrolytes exhibited good stability against lithium metal. However, their low oxidization stability has inhibited their development with high-voltage transition-metal oxide cathodes. Moreover, the low

https://doi.org/10.1021/accountsmr.1c00137
Acc. Mater. Res. 2022, 3, 21−32

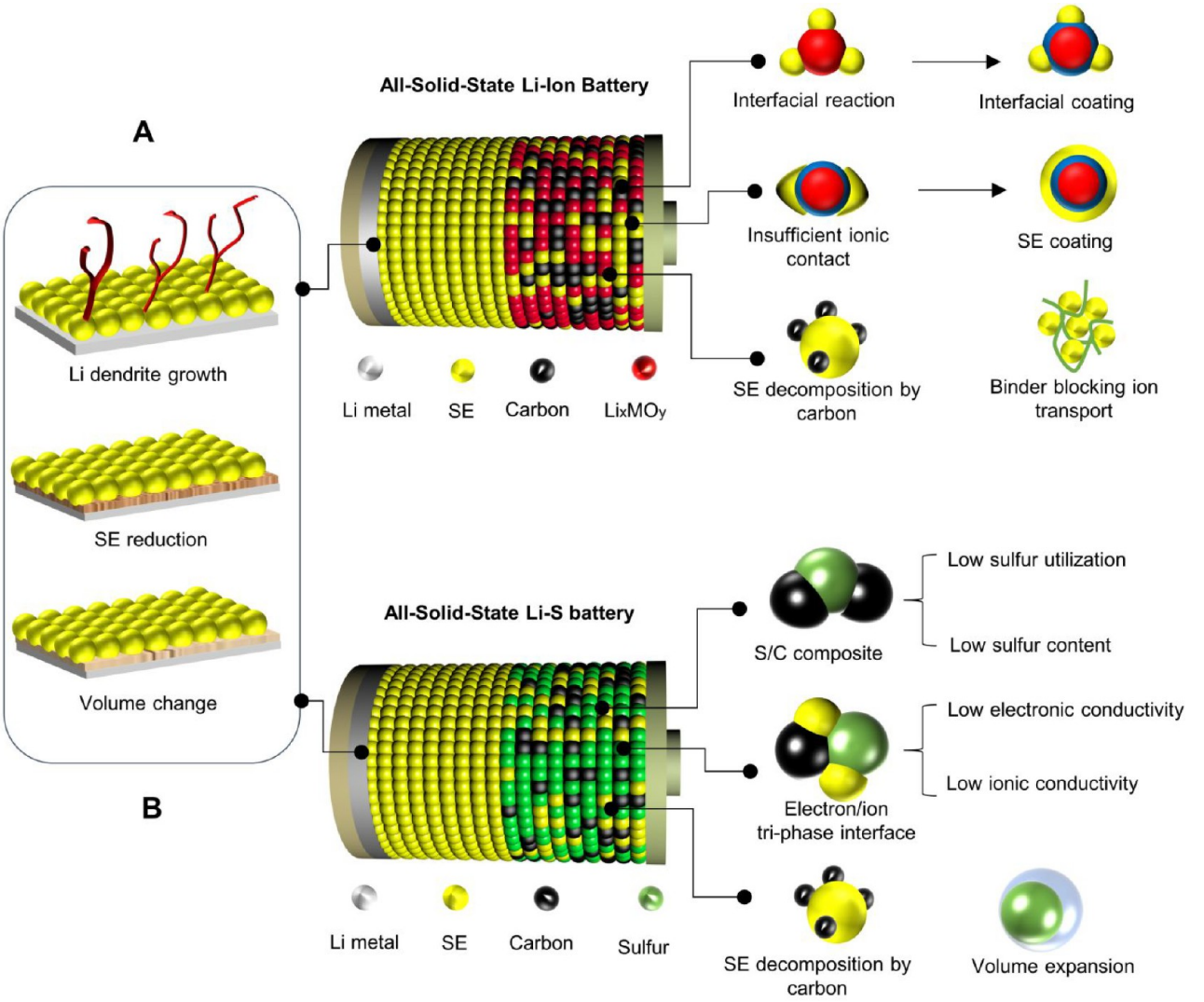

Figure 2. Schematic illustration of interface challenges of all-solid-state lithium metal batteries, including all-solid-state lithium−metal batteries and all-solid-state lithium−sulfur batteries.

thermal stability of solid-state borohydride electrolytes may limit the operating temperature window of ASSLMBs, which should be carefully evaluated in the future.

Along with the success of solid-state inorganic electrolytes, relentless effort has also been expended to develop organic solid-state polymer electrolytes. The solid-state polymer electrolytes have wide electrochemical windows, low cost, good flexibility, and low room-temperature ionic conductivity, these properties need to be further enhanced to develop ASSLMBs that can be operated under all weather conditions. Some quasi-solid-state polymer electrolytes can show a high ionic conductivity ($>10^{-4}$ $S{\cdot}cm^{-1}$). However, the safety and high-temperature stability of solid-state batteries with gel electrolytes cannot compete with inorganic counterparts. Taking into consideration that none of the solid-state electrolytes (SSEs) can meet all of the requirements for use in ASSLMBs, it is anticipated that the rational design of hybrid solid electrolytes may solve this dilemma in the near future,[24] which is beyond the scope of this Account.

Although they have high room-temperature ionic conductivity, SEs suffer from narrow electrochemical windows, which leads to considerably interfacial reactions against high voltage and lithium metal anodes. The considerable interfacial reactions in turn result in large interfacial resistance, thereby limiting interfacial electron and ion transport and suppressing the electrochemical performance of SE-based ASSLMBs. Our group has been dedicated to addressing the interfacial challenges of SE-based ASSLMBs for several years and has made some encouraging progress. In the following section, our recent understanding of interfacial electron and ion transport in SE-based ASSLIBs and ASSLSBs was discussed, respectively.

3. SUMMARY OF INTERFACIAL CHALLENGES OF SULFIDE-BASED ALL-SOLID-STATE LITHIUM METAL BATTERIES

As depicted in Figure 2A, directly using SEs to develop ASSLIBs with high-voltage transition-metal oxides (TMOs) (>4 V vs Li^+/Li) faces tremendous challenges. First, TMOs significantly react with SEs, leading to highly resistive interphases that block the interfacial ion and electron transport. Second, the large difference in the electrochemical potential of SEs and TMOs will lead to the formation of a lithium-ion depletion region at the interface, the so-called space−charge layer, which also considerably affects interfacial ion transport.[25] To prevent interfacial reactions and the space−charge effect, interfacial

https://doi.org/10.1021/accountsmr.1c00137
Acc. Mater. Res. 2022, 3, 21−32

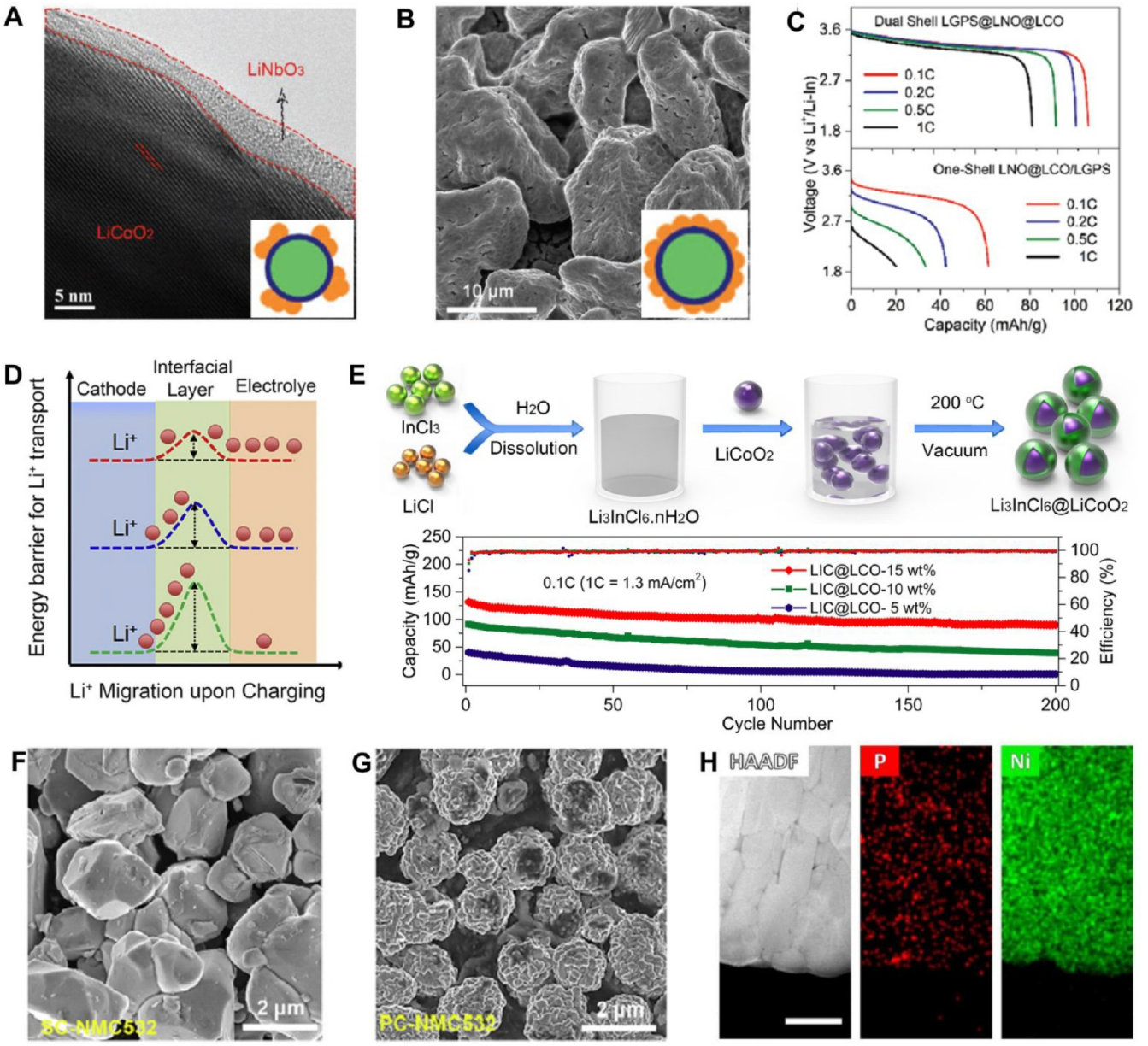

Figure 3. (A) TEM image of $LiNbO_3$-coated $LiCoO_2$ (core−shell LNO@LCO). (B) SEM image of $Li_{10}GeP_2S_{12}$ (LGPS) uniformly coated on $LiNbO_3$@$LiCoO_2$ (dual-shell LGPS@LNO@LCO). (C) Rate performance comparison between one-shell LNO@LCO/LGPS and dual-shell LGPS@LNO@LCO cathode composites. Reprinted with permission from ref 26. Copyright 2019, Wiley-VCH. (D) Impact of interfacial ionic conductivity on all-solid-state battery performance. Reprinted with permission from ref 37. Copyright 2020, Elsevier. (E) Interface-assisted in situ growth of Li_3InCl_6 on the $LiCoO_2$ surface. Reprinted with permission from ref 38. Copyright 2020, Elsevier. (F) SEM image of single-crystal NMC532. (G) SEM image of polycrystalline NMC532. Reprinted with permission from ref 39. Copyright 2020, Elsevier. (H) Dual-functional interface strategy to improve the NMC811 performance in all-solid-state batteries. Reprinted with permission from ref 40. Copyright 2020, Elsevier.

coatings between TMOs and SEs are a prerequisite. Third, the poor interfacial solid−solid ionic contact between TMOs and SEs significantly hinders interfacial ion transport and limits active material utilization.[26] To improve the interfacial solid−solid ionic contact, a solvent-involved process has been developed to uniformly coat SE on the electrode material surface, which improves the interfacial lithium-ion transport kinetics. Fourth, the conductive carbon agents in the cathode composites tend to decompose the SE during the charge/discharge process.[27,28] Therefore, rationally balancing interfacial ion and electron transport in the cathode composites is very crucial for SE-based ASSLIBs.[29] Finally, polymeric binders, which are normally required for fabricating the sheet-type electrodes for solid-state pouch cells, also block the lithium ion transport if a large amount is added.[30] These challenges must be addressed before the successful commercialization of ASSLMBs.

On the anode side, a lithium metal anode is the ultimate choice for realizing the high energy density because of its lowest potential (−3.040 V vs the standard hydrogen electrode) and largest specific capacity (3860 $mAh{\cdot}g^{-1}$).[31] However, tremendous challenges hindered the application of lithium metal in ASSLMBs, such as a low Coulombic efficiency, detrimental interfacial reactions between lithium metal and SEs, lithium dendrite growth, and infinite volume change, as illustrated in Figure 2.

https://doi.org/10.1021/accountsmr.1c00137
Acc. Mater. Res. 2022, 3, 21−32

Sulfur is a promising cathode material for developing high-energy-density Li−S batteries due to its high capacity (1672 $mAh{\cdot}g^{-1}$), low cost, abundance, and high sustainability. Unlike the high-voltage TMOs cathodes, sulfur cathodes are more chemically compatible with SEs due to their lower operation voltage ranges (1−3 V vs Li^+/Li).[32] When pairing with lithium metal anodes to form all-solid-state lithium−sulfur batteries (ASSLSBs), the theoretical energy density can reach as high as 2600 $Wh{\cdot}kg^{-1}$.[33−35] Therefore, SEs-based ASSLSBs have attracted intense research interest in recent years. However, the slow charge transfer kinetics and significant volume change (~80%) significantly hindered the development of SE-based ASSLSBs, which originate from the poor electrical conductivity of elemental sulfur (1.5×10^{-15} $S{\cdot}cm^{-1}$, density = 2.07 $g.cm^{-3}$) and their discharge product (Li_2S, 10^{-13} $S{\cdot}cm^{-1}$, 1.67 $g{\cdot}cm^{-3}$). To boost interfacial charge transfer, sulfur should be uniformly distributed in a conductive carbon matrix in which both high sulfur content and high sulfur utilization should be guaranteed for achieving a high energy density (Figure 2B). Simply increasing the electronic conductivity of sulfur cathodes cannot guarantee high-performance ASSLSBs because the cycling of sulfur cathodes also requires efficient ion transport. Therefore, a triphase interface among sulfur, conductive carbon, and SEs should be constructed to enable efficient electron and ion transport in sulfur cathodes, which is very critical for realizing high-performance ASSLSBs with both high energy density and high power density. In addition, minimizing the SE decomposition caused by conductive carbon and the significant volume change of sulfur cathodes upon cycling are another two challenges associated with sulfur cathodes.

On the basis of the aforementioned interfacial challenges, innovative strategies are required to overcome interfacial challenges and boost interfacial ion and electron transport. In the following sections, we summarize our recent understandings on interfacial ion and electron transport kinetics of both all-solid-state lithium ion batteries and next-generation solid-state lithium−sulfur batteries, which are categorized as (i) the TMO/SE interface, (ii) the sulfur/SE interface, and (iii) the Li/SE interface.

3.1. Regulating Interfacial Ion and Electron Transport between TMOs and SEs

To boost interfacial ion and electron transport at the TMO/SE interface, the interfacial reactions and space−charge effect should be suppressed while the solid−solid contact should be improved.[36] To this end, a dual-shell structure has been designed for cathode composites, in which an inner layer is devised to prevent the interfacial reactions and space−charge effect while the outer layer is used to realize intimate solid−solid ionic contact. To realize the inner layer, sol−gel or fluidized bed methods have been widely used. However, these methods cannot control the uniformity of the surface coating layer. Our group has pioneered the use of atomic layer deposition to deposit $LiNbO_3$ (LNO) on the $LiCoO_2$ (LCO) surface, which effectively suppressed the interfacial reactions due to the full coverage of LNO coatings (Figure 3A).[26] Furthermore, $Li_{10}GeP_2S_{12}$ (LGPS) was further dispersed on the LNO@LCO surface to improve the solid−solid ionic contact (Figure 3B). As a result, LGPS@LNO@LCO with a dual-shell interfacial structure LCO demonstrated a high capacity, negligible polarization, and excellent rate performance (Figure 3C). This dual-shell configuration demonstrates an ideal interfacial structure for realizing high-performance ASSLIBs. The ionic conductivity of the coating layer itself also makes a difference in the interfacial ion transport. To understand the effect of interfacial ionic conductivity on interfacial ion transport, we designed interfacial coating layers with various ionic conductivities. It is found that the higher ionic conductivity of the interfacial coatings shows a lower energy barrier for interfacial ion transport (Figure 3D),[37] which endows ASSLIBs with excellent rate performance. More importantly, the critical interfacial ionic conductivity of the coating layer should be less than 10^{-5} $S{\cdot}cm^{-1}$. To further verify the importance of interfacial ionic conductivity, a thin layer of Li_3InCl_6 (LIC) with high ionic conductivity (>1 $mS{\cdot}cm^{-1}$) in situ grew on the LCO surface (Figure 3E). Owing to the strong interfacial interaction, high interfacial ionic conductivity (>1 mS cm^{-1}), and excellent interfacial compatibility, LCO with 15 wt % LIC exhibits a high initial capacity of 131.7 $mAh{\cdot}g^{-1}$ at 0.1C (1C = 1.3 $mA{\cdot}cm^{-2}$) and can be operated to up to 4C at room temperature.[38] This research progress suggests that boosting the interfacial lithium ion transport is paramount for realizing high-performance ASSLIBs.

In addition to the interfacial ion transport, electron transport is also extremely crucial for the TMO/SE cathode composites. To enable fast interfacial electron transport, conductive carbon additives are added to increase the electronic conductivity. However, carbon additives generally decompose solid-state SEs, which is harmful to the electrochemical performance of ASSLIBs.[27] To address this issue, we have devised PEDOT-coated carbon nanotubes (PEDOT@CNTs) as the conductive agents to boost the electrons in the cathode composites, which also effectively alleviated the side reactions between the carbon and SEs.[28]

The stress and strain induced by the TMO volume change is another critical challenge in SE-based ASSLIBs. The first solution is to use single-crystal TMO materials in ASSLIBs, which can reduce the internal stress upon cycling and enable fast ion transport kinetics.[41,42] As shown in Figure 3F,G, we have systematically compared single-crystal $LiNi_{0.5}Mn_{0.3}Co_{0.2}O_2$ (NMC532) with its polycrystalline counterpart, and it was found that single-crystal NMC532 possess fast ion transport kinetics as well as good tolerance to stress upon cycling in ASSLIBs.[39] The second solution is to tailor a dual-function interface[40,43] in which a surface coating was diffused into the grain boundaries of secondary polycrystalline particles via postannealing. This grain boundary engineering effectively alleviates intergranular cracking and the layered-to-spinel phase transformation. To verify this, a dual-function solid Li_3PO_4 (LPO) electrolyte was infused into the grain boundaries of polycrystalline $LiNi_{0.8}Mn_{0.1}Co_{0.1}O_2$ (NMC811) (Figure 3H). After thermal infusion, the surface was further covered by LPO to prevent interfacial reactions between NMC811 and SEs. It was found that the dual-function LPO modification not only significantly suppresses the side reactions with SEs but also helps to alleviate the deterioration of the microstructural cracks.[40] The advances in the cathode interface design provide several indications: First, an interfacial coating layer with high ionic conductivity is required to ensure fast ion transport with low energy barriers. Second, carbon additives should be added to provide sufficient interfacial electron transport providing that SE decomposition by carbon is well-balanced. Third, the significant stress/strain induced by the volume change of cathode particles upon cycling should be tailored either by using a single-crystal TMO cathode and grain boundary engineering.

https://doi.org/10.1021/accountsmr.1c00137
Acc. Mater. Res. 2022, 3, 21−32

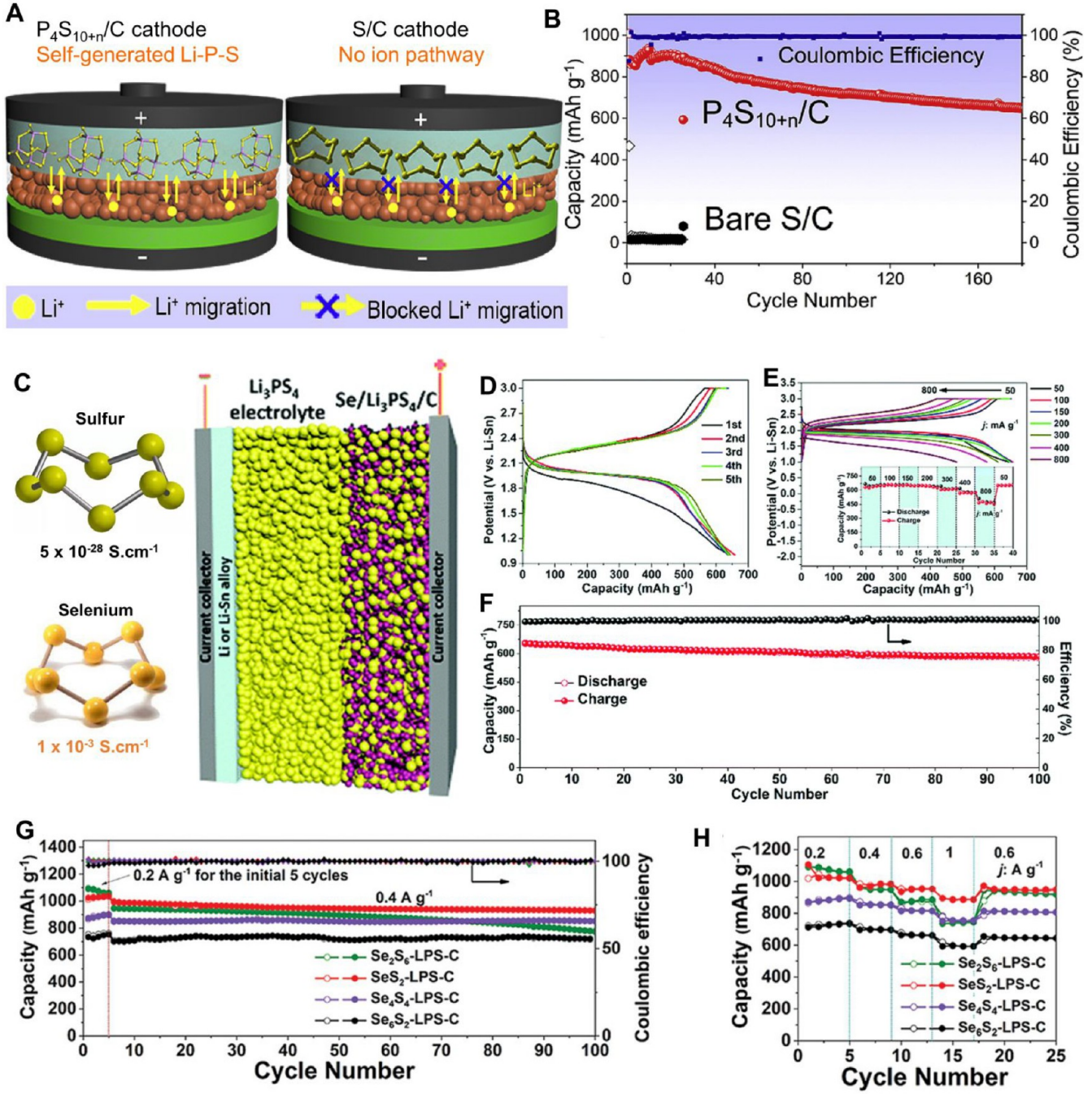

Figure 4. (A) Schematic illustration of SE-based all-solid-state lithium−sulfur batteries with P_4S_{10+n} cathodes, which was enabled by self-generated lithium ion pathways. (B) Long-term cycling stability of P_4S_{10+n}/C cathodes. Reprinted with permission from ref 46. Copyright 2020, Elsevier. (C) Illustration of all-solid-state lithium−selenium batteries highlighting the significantly higher electronic conductivity of selenium compared to that of elemental sulfur. (D) Discharge/charge curves of the Se/Li_3PS_4/Li−Sn all-solid-state cell at 50 mA g^{-1}. (E) Representative discharge/charge curves at different current densities (inset: rate performance at current densities ranging from 50 to 800 mA·g^{-1}). (F) Cycling performance at 50 mA g^{-1} and corresponding Coulombic efficiencies. Reprinted with permission from ref 47. Copyright 2018, Royal Society of Chemistry. (G) Cycling performance of SeSx−LPS−C cathodes at 0.4 A·g^{-1} at 60 °C. (H) Rate capability of SeSx−LPS−C cathodes at different current densities from 0.2 to 1 A·g^{-1} at 60 °C. Reprinted with permission from ref 32. Copyright 2019, Wiley-VCH.

3.2. Understanding Interfacial Ion and Electron Transport between Sulfur and SEs

Compared to ASSLIBs, all-solid-state lithium−sulfur batteries (ASSLSBs) could achieve a much higher energy density beyond 500 Wh·kg^{-1}, which is therefore regarded as the most promising energy storage technology.[31,34,44,45] The fatal weaknesses of ASSLSBs are poor lithium ion (Li^+) and electron transport between sulfur and SEs, which arises from the low electronic conductivity of elemental sulfur and discharge product Li_2S, SE decomposition by carbon, and the significant volume change. Therefore, it is critical to construct a triphase interface among the sulfur cathode, SEs, and conductive carbon matrix for ASSLSBs, which can facilitate the high Li^+ and electron transport simultaneously. With this understanding, our group first synthesized a series of unique P_4S_{10+n} cathodes for high-

https://doi.org/10.1021/accountsmr.1c00137
Acc. Mater. Res. 2022, 3, 21−32

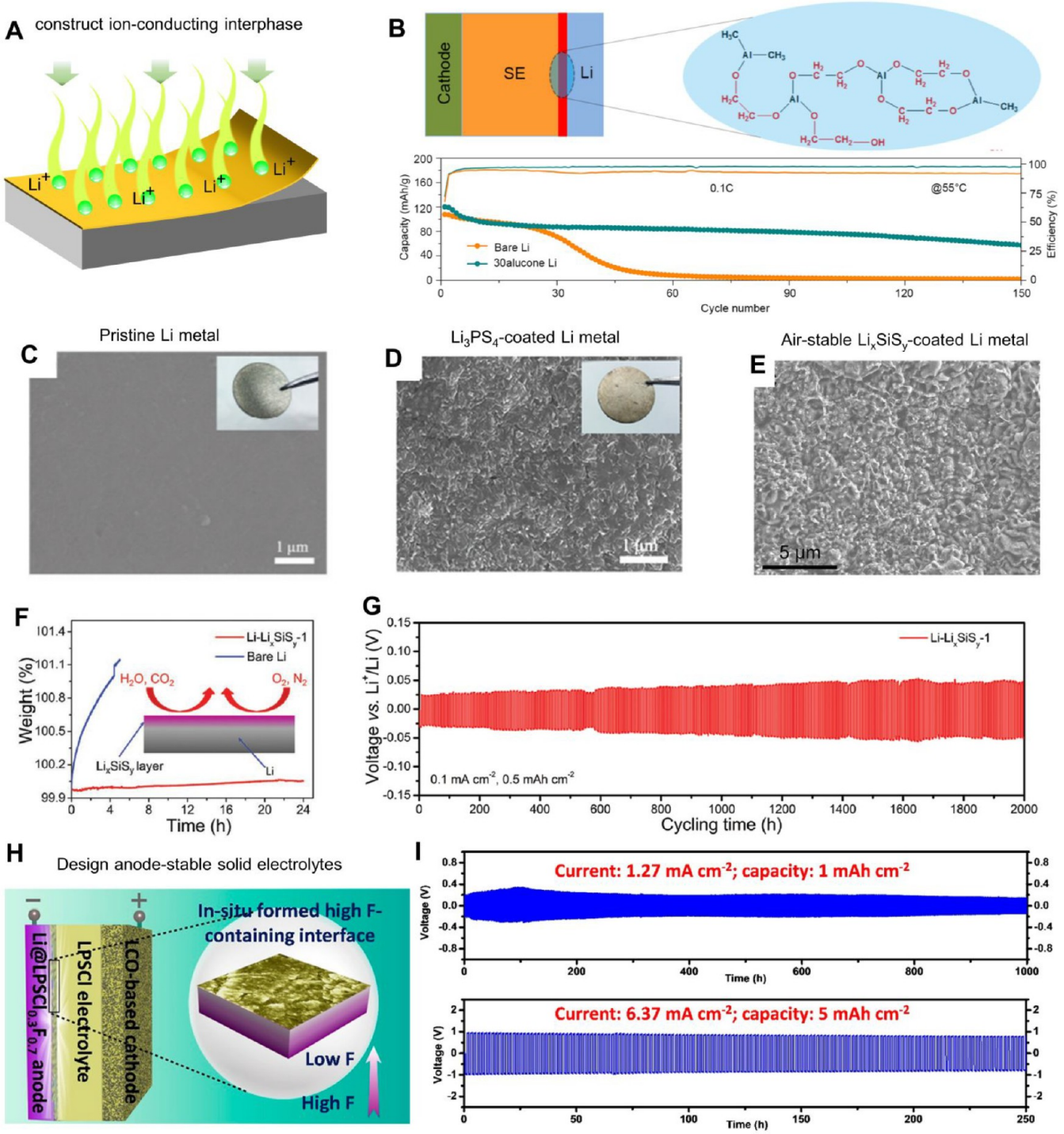

Figure 5. (A) Constructing an artificial SEI for the lithium metal anode in ASSLMBs. (B) An inorganic and organic hybrid interface was deposited on a lithium metal surface via molecular-layer deposition (MLD). (C) SEM image of a pristine lithium metal surface. Reprinted with permission from ref 56. Copyright 2018, Elsevier. (D) SEM image of a Li_3PS_4-decorated lithium metal surface. (E) SEM image of a Li_xSiS_y-coated lithium metal surface. Reprinted with permission from ref 57. Copyright 2018, Wiley-VCH. (F) TGA profiles of Li_xSiS_y-coated lithium metal. (G) Long-term cycling stability of symmetric cells with the structure of Li-Li_xSiS_y-Li_3PS_4-Li_xSiS_y-Li with a capacity of 0.5 mAh·cm^{-2}. Reprinted with permission from ref 58. Copyright 2019, Wiley-VCH. (H) Schematic diagram of the Li@$LPSCl_{0.3}F_{0.7}$/LPSCl//LCO@LNO/LPSCl ASSLMBs with the highlighted fluorinated interface layer. (I) Current density (1.27 mA·cm^{-2}) and cutoff capacity (1 mAh·cm^{-2}). Current density (6.37 mA·cm^{-2}) and cutoff capacity (5 mAh·cm^{-2}). Reprinted with permission from ref 59. Copyright 2020, ACS.

performance SE-based ASSLSBs. Synchrotron-based X-ray absorption near-edge structure and Raman analyses indicate that ionically conductive Li_3PS_4 together with $Li_4P_2S_6$ components can be self-generated electrochemically during the initial lithiation process, which can effectively conduct a lithium ion inside C/P_4S_{10+n} cathodes (Figure 4A). As a result, P_4S_{34}/C-based ASSLSBs show a highly reversible capacity of 883 mAh·g^{-1} and stable cycling performance over 180 cycles with a high active material content of 70 wt % (Figure 4B).[46] This strategy of self-generating ion-conductive pathways from

https://doi.org/10.1021/accountsmr.1c00137
Acc. Mater. Res. 2022, 3, 21−32

the electrode itself can effectively facilitate Li^+ migration within electrodes in ASSLSBs. Second, compared to sulfur, selenium (Se) has a much higher electronic conductivity (1×10^{-3} vs 5×10^{-28} S·cm^{-1} at room temperature). Therefore, Se should have much better electrochemical kinetics than sulfur due to its fast charge transfer capability. For this reason, all-solid-state Li−Se batteries were successfully constructed for the first time.[47] Significant improvements in both ionic and electronic conductivities of the cathode were achieved by ball-milling Se, Li_3PS_4, and acetylene black, which facilitate the fast ion transport and feasible charge transfer during electrochemical reaction processes. Specifically, Li^+ transport over the Se−Li_3PS_4 interface is as high as 1.4×10^{-5} S·cm^{-1}. As a result, all-solid-state Li−Se batteries with a configuration of Se/Li_3PS_4/Li−Sn delivered a high reversible capacity of 652 mAh·g^{-1} at 50 mA·g^{-1}, achieving 96% of the theoretical capacity. In addition, the initial Coulombic efficiency is as high as 97% in the first cycle (Figure 4D). Moreover, high reversible capacities of 652, 649, 642, 611, 574, and 462 mAh·g^{-1} were attained under current densities of 100, 150, 200, 300, 400, and 800 mA g^{-1}, respectively (Figure 4E). Figure 4F also demonstrated the ultrastable cycling performance of all-solid-state Li−Se batteries. A capacity of 585 mAh·g^{-1} and a correspondingly retention of 90% were retained after 100 cycles, indicating that the large volume change of the Se cathode was successfully minimized via external pressure.

Even though all-solid-state Li−Se batteries demonstrated superb electrochemical performance, selenium has a lower specific capacity (680 mAh·g^{-1}) than the high theoretical capacity (1672 mAh·g^{-1}) of sulfur, which is not beneficial to achieving a high energy density. To further improve the energy density of ASSLSBs, we developed a series of Se−S solid solutions. By introducing Se into sulfur to form SeS_x solid solutions, the electrochemical reaction kinetics and active material utilization could be significantly improved.[32] As a result, the reversible capacities obtained at the fifth cycle were 1086, 1116, 883, and 733 mAh·g^{-1} for SeS_x solid solutions with increasing Se content, corresponding to 87, 99, 91, and 90% of the theoretical specific capacities (Figure 4G). Figure 4H shows the rate capabilities of the SeS_x−LPS−C cathodes over a current density range from 0.2 to 1 A·g^{-1}. The SeS_2−LPS−C cathode exhibited the best rate capability, with high reversible capacities of 1024, 970, 949, and 887 mAh·g^{-1} achieved at 0.2, 0.4, 0.6, and 1 A·g^{-1}, respectively. Moreover, high-loading cells can achieve high areal capacities of up to 12.6 mAh·cm^{-2}. As confirmed by the experimental results, the ionic and electronic conductivities of the SeS_x−Li_3PS_4−C cathodes can be favorably tuned by the ratio of Se to S in SeS_x solid solutions. This work deepens the understanding of Se−S solid solution chemistry and offers a new strategy to achieve high-performance S-based cathodes for application in ASSLSBs.

As a brief summary, our group has developed high-performance ASSLSBs via self-generating Li^+ conductive pathways inside the C/P_4S_{10+n} cathode, used electronically conductive Se as the cathode, and synthesized Se−S solid solutions to regulate interfacial Li^+ and electron transport. Several important conclusions can be drawn from these works:[48−51] (i) the triphase interface among sulfur, SE, and the conductive agent should be sufficiently constructed to ensure high active material utilization; (ii) improving the electronic and ionic conductivities of cathode composites is very crucial for fast interfacial charge transfer; and (iii) external pressure is normally required to suppress the significant volume change of sulfur cathodes upon cycling.

3.3. Understanding Interfacial Lithium Ion Transport between Li Metal and SEs

To address the challenges between Li metal and SEs, the most common strategy is to construct an artificial solid electrolyte interphase (SEI) (Figure 5A)[52] which allows fast interfacial Li^+ transport but blocks electron transport. Thus, interfacial reactions between Li metal and SE can be avoided. In addition, the fast Li^+ transport capability of the SEI can realize homogeneous Li^+ deposition, thus alleviating lithium dendrite growth. Following this strategy, we have designed an inorganic and organic interfacial layer (i.e., alucone) by molecular layer deposition (Figure 5B), which not only suppressed the reduction of $Li_{10}SnP_2S_{12}$ by lithium metal but also inhibited the lithium dendrite growth. As a result, ASSLMBs with the alucone-coated lithium metal anode demonstrated an elongated cycling life. Furthermore, we have chemically modified pristine lithium with P_4S_{16}/NMP (*N*-methyl-2-pyrrolidone) solutions. Because of the self-limiting reactions between P_4S_{16} and Li NMP, a lithium ion conductive Li_3PS_4 with a thickness of 60 nm was formed in situ on the Li metal surface (Figure 5C,D). Because of the high ionic conductivity and low electronic conductivity of Li_3PS_4, the intimate protection layer of Li_3PS_4 not only prevented the formation of Li dendrites but also suppressed interfacial side reactions and improved the electrochemical performance. Although the Li_3PS_4 thin film exhibits high ionic conductivity, they have poor air stability and are not favorable for processing lithium foil in a dry room. We further developed an air-stable Li_xSiS_y-coated lithium metal via the chemical reactions among Li_2S_8, $SiCl_4$, and Li. As shown in Figure 5E, porous Li_xSiS_y was used to decorate the Li metal surface. Because the Li_xSiS_y layer is chemically inert, impermeable to dry air, and robust against oxidation, Li_xSiS_y-coated lithium metal demonstrated excellent air stability in an ambient environment, which was confirmed by thermal gravimetric analysis (TGA) in Figure 5F. The Li_xSiS_y-coated lithium metal shows a slight weight increase within 24 h, implying that the parasitic side reaction between Li metal and dry air is effectively blocked by the Li_xSiS_y coating layer. In terms of electrochemical performance, highly stable Li cycling for over 2000 h in symmetrical cells was achieved with a capacity of 0.5 mAh·cm^{-2} (Figure 5G). Meanwhile, we also have developed a gradient interfacial SEI layer by rationally using advanced atomic layer deposition (ALD) and molecular layer deposition (MLD).[52,53]

Apart from the rational design of an artificial SEI layer on a lithium metal surface, tailoring SE composition, such as through introducing halide elements (e.g., F, I) into SEs also can effectively suppress lithium dendrite formation in ASSLMBs by in-situ-formed SEI. For example, we have synthesized a fluorinated SE with a chemical formula of $Li_6PS_5Cl_{0.4}F_{0.7}$ which can react with Li metal during the Li^+ platting and stripping process. As a result, a highly fluorinated interface was formed in situ on the Li metal surface (Figure 5H). This highly fluorinated interface can serve as an SEI, stopping further interfacial reactions and suppressing lithium dendrite growth. As a result, all-solid-state lithium symmetric cells with a configuration of Li/Li $Li_6PS_5Cl_{0.4}F_{0.7}$/Li can be stable even under a large current density (6.37 mA·cm^{-2}) with a large capacity of 5 mAh·cm^{-2}. Furthermore, the introduction of iodine into the SE also can produce an iodinated interface

https://doi.org/10.1021/accountsmr.1c00137
Acc. Mater. Res. 2022, 3, 21−32

between the Li metal and SEs.[20] Under a high current density of 1.26 mA·cm^{-2} and a cutoff capacity of 1 mAh·cm^{-2}, the Li/$Li_{6.24}P_{0.823}Sn_{0.177}S_{4.58}I_{0.9}$/Li symmetric cell can still display very stable Li plating and stripping behavior for 200 h (125 cycles) at room temperature. We believe that this strategy can be transferred to other halide elements, including Br, Cl, and even binary halide electrolytes.

In summary, constructing an interfacial SEI layer on the Li metal surface and tailoring the SE composition to form a stable SEI in situ can overcome the interfacial challenges between Li metal and SE to some extent. However, the current density and cycling capacity of most Li/SE/Li symmetrical cells reported in previous work are limited and far from the practical requirements. To the best of our knowledge, a large areal capacity of 4 mAh·cm^{-2} is required to realize a high energy density. In addition, ultrathin Li metal (<40 μm) instead of thick lithium foil (~460 μm) is suggested for future studies.[54,55] More importantly, both the suppression of the lithium dendrite growth and the high Coulombic efficiency (>99.98%) of ultrathin Li metal are important for ASSLMB's long cycle life. To address the volume change issues of ASSLMBs, external pressure should be optimized without compromising the cost and high energy density. The high Coulombic efficiency of ultrathin Li is a prerequisite for the long lifespan of ASSLMBs.

4. SUMMARY AND PERSPECTIVES

In this Account, we provided a systematic review of our recent progress on the interface understanding of ASSLMBs with SEs. First, the advantages of SEs over other solid-state electrolytes were presented, particularly their outstanding RT ionic conductivity. Then, interfacial challenges of SE-based ASSLIBs and ASSLSBs were summarized, including their detrimental interfacial reactions, space−charge layer, poor solid−solid ionic contact, considerable volume change, and lithium dendrite growth. At the TMO/SE interface, we have proposed a series of innovative strategies, including designing an interfacial coating layer with high ionic conductivity and good conformability, engineering a core−shell−shell interfacial nanostructure, using single-crystal TMOs cathodes, and minimizing the detrimental effect of carbon additives. These innovative interfacial approaches significantly facilitate the interfacial ion and electron transport, enabling high-performance SE-based ASSLIBs. At the triphase interface among conductive carbon, sulfur, and SEs, ultrafast electron and ion transport were realized via self-generating Li^+ conductive pathways inside C/P_4S_{10+n} cathodes using high electronically conductive Se as the cathode and regulating Se−S solid solutions. At the Li/SE interface, the design of an artificial SEI layer via self-limiting reactions or atomic/molecular layer deposition as well as tailoring SE composition through introducing halide elements (e.g., F, I) can form a stable SEI between Li and SEs.

Although innovative interfacial strategies can successfully demonstrate high-performance SE-based ASSLMBs, further effort is still required in the coming years to realize their successful commercialization. First, continuous research effort on accelerating the interfacial ion and electron transport is still necessary, particularly for high-energy-density SEs-based ASSLMBs based on thick cathode composites (≥4 mAh·cm^{-2}) and ultrathin Li metal (≤40 μm). Second, the significant volume change of SE-based ASSLMBs should be accommodated via rational interface design, material advances, and even optimal external stacking pressure. Third, the high stacking pressure needs to be reduced to meet the practical application requirements. Fourth, advanced characterizations and theoretical calculations are highly recommended to better understand the interfacial ion and electron transport process with more realistic parameters. Finally, lowering the material price and fabrication cost is also crucial to the commercial success of SE-based ASSLMBs. We believe that the continuous advances in solid-state electrolytes and ASSLMBs will eventually lead to their great success in the market.

AUTHOR INFORMATION

Corresponding Author

Xueliang Sun − *Department of Mechanical & Materials Engineering, University of Western Ontario, London, ON N6A 5B9, Canada*; orcid.org/0000-0003-0374-1245; Email: xsun9@uwo.ca

Authors

Changhong Wang − *Department of Mechanical & Materials Engineering, University of Western Ontario, London, ON N6A 5B9, Canada*

Keegan Adair − *Department of Mechanical & Materials Engineering, University of Western Ontario, London, ON N6A 5B9, Canada*

Complete contact information is available at: https://pubs.acs.org/10.1021/accountsmr.1c00137

Notes

The authors declare no competing financial interest.

Biographies

Changhong Wang is currently serving as the R&D director of GLABAT Solid-State Battery Inc. in Canada. He received his Ph.D. in mechanical and materials engineering from the University of Western Ontario (UWO) in 2020 and his M.S. in materials engineering from the University of Science and Technology of China (USTC) in 2014. Changhong has worked at the Singapore University of Technology and Design (SUTD) from 2014 to 2016, focusing on electronic synapses for neuromorphic computing. His current research interests include solid-state batteries, solid electrolytes, pouch cell engineering, and brain-inspired devices.

https://doi.org/10.1021/accountsmr.1c00137
Acc. Mater. Res. 2022, 3, 21−32

Keegan Adair received his B.Sc. in chemistry from the University of British Columbia in 2016. He is currently a Ph.D. candidate in Prof. Xueliang (Andy) Sun's nanomaterials and energy group at the University of Western Ontario, Canada. Keegan has previously worked on battery technology at companies such as E-One Moli Energy and General Motors. His research interests include the design of nanomaterials for lithium metal batteries and nanoscale interfacial coatings for battery applications.

Xueliang (Andy) Sun is a Canada Research Chair in the Development of Nanomaterials for Clean Energy, a Fellow of the Royal Society of Canada and the Canadian Academy of Engineering, and a full professor at the University of Western Ontario, Canada. Dr. Sun received his Ph.D. in materials chemistry in 1999 from the University of Manchester, U.K., which he followed up by working as a postdoctoral fellow at the University of British Columbia and as a research associate at L'Institut National de la Recherche Scientifique (INRS), Canada. His current research interests are focused on advanced materials for electrochemical energy storage and conversion.

■ ACKNOWLEDGMENTS

This research was supported by the Natural Sciences and Engineering Research Council of Canada (NSERC), the Canada Research Chair Program (CRC), the Canada Foundation for Innovation (CFI), the Ontario Research Fund, and the University of Western Ontario.

■ REFERENCES

(1) Liang, J.; Chen, N.; Li, X.; Li, X.; Adair, K. R.; Li, J.; Wang, C.; Yu, C.; Norouzi Banis, M.; Zhang, L. Li10Ge (P1−x Sb x) 2S12 Lithium-Ion Conductors with Enhanced Atmospheric Stability. *Chem. Mater.* **2020**, *32*, 2664−2672.

(2) Asano, T.; Sakai, A.; Ouchi, S.; Sakaida, M.; Miyazaki, A.; Hasegawa, S. Solid Halide Electrolytes with High Lithium-Ion Conductivity for Application in 4 V Class Bulk-Type All-Solid-State Batteries. *Adv. Mater.* **2018**, *30*, 1803075.

(3) Li, X.; Liang, J.; Chen, N.; Luo, J.; Adair, K. R.; Wang, C.; Banis, M. N.; Sham, T. K.; Zhang, L.; Zhao, S. Water-Mediated Synthesis of a Superionic Halide Solid Electrolyte. *Angew. Chem.* **2019**, *131*, 16579−16584.

(4) Liang, J.; Li, X.; Adair, K. R.; Sun, X. Metal Halide Superionic Conductor for All-Solid-State Batteries. *Acc. Chem. Res.* **2021**, *54*, 1023−1033.

(5) Li, X.; Liang, J.; Luo, J.; Norouzi Banis, M.; Wang, C.; Li, W.; Deng, S.; Yu, C.; Zhao, F.; Hu, Y.; Sham, T.-K.; Zhang, L.; Zhao, S.; Lu, S.; Huang, H.; Li, R.; Adair, K. R.; Sun, X. Air-stable Li3InCl6 electrolyte with high voltage compatibility for all-solid-state batteries. *Energy Environ. Sci.* **2019**, *12*, 2665−2671.

(6) Li, X.; Liang, J.; Yang, X.; Adair, K. R.; Wang, C.; Zhao, F.; Sun, X. Progress and perspectives on halide lithium conductors for all-solid-state lithium batteries. *Energy Environ. Sci.* **2020**, *13*, 1429−1461.

(7) Wang, C.; Liang, J.; Luo, J.; Liu, J.; Li, X.; Zhao, F.; Li, R.; Huang, H.; Zhao, S.; Zhang, L.; Wang, J.; Sun, X. A universal wet-chemistry synthesis of solid-state halide electrolytes for all-solid-state lithium-metal batteries. *Sci. Adv.* **2021**, *7*, DOI: 10.1126/sciadv.abh1896.

(8) Zhang, J.; Zhao, J.; Yue, L.; Wang, Q.; Chai, J.; Liu, Z.; Zhou, X.; Li, H.; Guo, Y.; Cui, G.; Chen, L. Safety-Reinforced Poly(Propylene Carbonate)-Based All-Solid-State Polymer Electrolyte for Ambient-Temperature Solid Polymer Lithium Batteries. *Adv. Energy Mater.* **2015**, *5*, 1501082.

(9) Liang, J.; Chen, D.; Adair, K.; Sun, Q.; Holmes, N. G.; Zhao, Y.; Sun, Y.; Luo, J.; Li, R.; Zhang, L. Insight into Prolonged Cycling Life of 4 V All-Solid-State Polymer Batteries by a High-Voltage Stable Binder. *Adv. Energy Mater.* **2021**, *11*, 2002455.

(10) Maekawa, H.; Matsuo, M.; Takamura, H.; Ando, M.; Noda, Y.; Karahashi, T.; Orimo, S.-i Halide-Stabilized LiBH4, a Room-Temperature Lithium Fast-Ion Conductor. *J. Am. Chem. Soc.* **2009**, *131*, 894−895.

(11) Kim, S.; Oguchi, H.; Toyama, N.; Sato, T.; Takagi, S.; Otomo, T.; Arunkumar, D.; Kuwata, N.; Kawamura, J.; Orimo, S.-i A complex hydride lithium superionic conductor for high-energy-density all-solid-state lithium metal batteries. *Nat. Commun.* **2019**, *10*, 1081.

(12) Zhu, Y.; He, X.; Mo, Y. First principles study on electrochemical and chemical stability of solid electrolyte−electrode interfaces in all-solid-state Li-ion batteries. *J. Mater. Chem. A* **2016**, *4*, 3253−3266.

(13) Wang, S.; Bai, Q.; Nolan, A. M.; Liu, Y.; Gong, S.; Sun, Q.; Mo, Y. Lithium Chlorides and Bromides as Promising Solid-State Chemistries for Fast Ion Conductors with Good Electrochemical Stability. *Angew. Chem., Int. Ed.* **2019**, *58*, 8039−8043.

(14) Zhu, Y.; He, X.; Mo, Y. Origin of Outstanding Stability in the Lithium Solid Electrolyte Materials: Insights from Thermodynamic Analyses Based on First-Principles Calculations. *ACS Appl. Mater. Interfaces* **2015**, *7*, 23685−23693.

(15) Wang, C.; Sun, Q.; Liu, Y.; Zhao, Y.; Li, X.; Lin, X.; Banis, M. N.; Li, M.; Li, W.; Adair, K. R.; Wang, D.; Liang, J.; Li, R.; Zhang, L.; Yang, R.; Lu, S.; Sun, X. Boosting the performance of lithium batteries with solid-liquid hybrid electrolytes: Interfacial properties and effects of liquid electrolytes. *Nano Energy* **2018**, *48*, 35−43.

(16) Liu, Y.; Sun, Q.; Zhao, Y.; Wang, B.; Kaghazchi, P.; Adair, K. R.; Li, R.; Zhang, C.; Liu, J.; Kuo, L.-Y.; Hu, Y.; Sham, T.-K.; Zhang, L.; Yang, R.; Lu, S.; Song, X.; Sun, X. Stabilizing the Interface of NASICON Solid Electrolyte against Li Metal with Atomic Layer Deposition. *ACS Appl. Mater. Interfaces* **2018**, *10*, 31240−31248.

(17) Kamaya, N.; Homma, K.; Yamakawa, Y.; Hirayama, M.; Kanno, R.; Yonemura, M.; Kamiyama, T.; Kato, Y.; Hama, S.; Kawamoto, K.; Mitsui, A. A lithium superionic conductor. *Nat. Mater.* **2011**, *10*, 682−686.

(18) Kato, Y.; Hori, S.; Saito, T.; Suzuki, K.; Hirayama, M.; Mitsui, A.; Yonemura, M.; Iba, H.; Kanno, R. High-power all-solid-state batteries using sulfide superionic conductors. *Nat. Energy* **2016**, *1*, 16030.

(19) Zhao, F.; Alahakoon, S. H.; Adair, K.; Zhang, S.; Xia, W.; Li, W.; Yu, C.; Feng, R.; Hu, Y.; Liang, J.; Lin, X.; Zhao, Y.; Yang, X.; Sham, T.-K.; Huang, H.; Zhang, L.; Zhao, S.; Lu, S.; Huang, Y.; Sun, X. An Air-

Stable and Li-Metal-Compatible Glass-Ceramic Electrolyte enabling High-Performance All-Solid-State Li Metal Batteries. *Adv. Mater.* **2021**, *33*, 2006577.
(20) Zhao, F.; Liang, J.; Yu, C.; Sun, Q.; Li, X.; Adair, K.; Wang, C.; Zhao, Y.; Zhang, S.; Li, W.; Deng, S.; Li, R.; Huang, Y.; Huang, H.; Zhang, L.; Zhao, S.; Lu, S.; Sun, X. A Versatile Sn-Substituted Argyrodite Sulfide Electrolyte for All-Solid-State Li Metal Batteries. *Adv. Energy Mater.* **2020**, *10*, 1903422.
(21) Li, X.; Liang, J.; Adair, K. R.; Li, J.; Li, W.; Zhao, F.; Hu, Y.; Sham, T.-K.; Zhang, L.; Zhao, S.; Lu, S.; Huang, H.; Li, R.; Chen, N.; Sun, X. Origin of Superionic Li3Y1−xInxCl6 Halide Solid Electrolytes with High Humidity Tolerance. *Nano Lett.* **2020**, *20*, 4384−4392.
(22) Liang, J.; Li, X.; Wang, S.; Adair, K. R.; Li, W.; Zhao, Y.; Wang, C.; Hu, Y.; Zhang, L.; Zhao, S. Site-Occupation-Tuned Superionic LixScCl3+ x Halide Solid Electrolytes for All-Solid-State Batteries. *J. Am. Chem. Soc.* **2020**, *142*, 7012−7022.
(23) Yu, C.; Li, Y.; Adair, K. R.; Li, W.; Goubitz, K.; Zhao, Y.; Willans, M. J.; Thijs, M. A.; Wang, C.; Zhao, F. Tuning ionic conductivity and electrode compatibility of Li3YBr6 for high-performance all solid-state Li batteries. *Nano Energy* **2020**, *77*, 105097.
(24) Liang, J.; Luo, J.; Sun, Q.; Yang, X.; Li, R.; Sun, X. Recent progress on solid-state hybrid electrolytes for solid-state lithium batteries. *Energy Storage Mater.* **2019**, *21*, 308−334.
(25) Wang, L.; Xie, R.; Chen, B.; Yu, X.; Ma, J.; Li, C.; Hu, Z.; Sun, X.; Xu, C.; Dong, S.; Chan, T.-S.; Luo, J.; Cui, G.; Chen, L. In-situ visualization of the space-charge-layer effect on interfacial lithium-ion transport in all-solid-state batteries. *Nat. Commun.* **2020**, *11*, 5889.
(26) Wang, C.; Li, X.; Zhao, Y.; Banis, M. N.; Liang, J.; Li, X.; Sun, Y.; Adair, K. R.; Sun, Q.; Liu, Y.; Zhao, F.; Deng, S.; Lin, X.; Li, R.; Hu, Y.; Sham, T.-K.; Huang, H.; Zhang, L.; Yang, R.; Lu, S.; Sun, X. Manipulating Interfacial Nanostructure to Achieve High-Performance All-Solid-State Lithium-Ion Batteries. *Small Methods* **2019**, *3*, 1900261.
(27) Zhang, W.; Leichtweiß, T.; Culver, S. P.; Koerver, R.; Das, D.; Weber, D. A.; Zeier, W. G.; Janek, J. The detrimental effects of carbon additives in $Li_{10}GeP_2S_{12}$-based solid-state batteries. *ACS Appl. Mater. Interfaces* **2017**, *9*, 35888−35896.
(28) Deng, S.; Sun, Y.; Li, X.; Ren, Z.; Liang, J.; Doyle-Davis, K.; Liang, J.; Li, W.; Norouzi Banis, M.; Sun, Q.; Li, R.; Hu, Y.; Huang, H.; Zhang, L.; Lu, S.; Luo, J.; Sun, X. Eliminating the Detrimental Effects of Conductive Agents in Sulfide-Based Solid-State Batteries. *ACS Energy Lett.* **2020**, *5*, 1243−1251.
(29) Pang, Y.; Pan, J.; Yang, J.; Zheng, S.; Wang, C. Electrolyte/Electrode Interfaces in All-Solid-State Lithium Batteries: A Review. *Electrochem. Energy Rev.* **2021**, *4*, 169−193.
(30) Hippauf, F.; Schumm, B.; Doerfler, S.; Althues, H.; Fujiki, S.; Shiratsuchi, T.; Tsujimura, T.; Aihara, Y.; Kaskel, S. Overcoming binder limitations of sheet-type solid-state cathodes using a solvent-free dry-film approach. *Energy Storage Mater.* **2019**, *21*, 390−398.
(31) Wang, C.; Liang, J.; Zhao, Y.; Zheng, M.; Li, X.; Sun, X. All-solid-state lithium batteries enabled by sulfide electrolytes: from fundamental research to practical engineering design. *Energy Environ. Sci.* **2021**, *14*, 2577.
(32) Li, X.; Liang, J.; Luo, J.; Wang, C.; Li, X.; Sun, Q.; Li, R.; Zhang, L.; Yang, R.; Lu, S. High-Performance Li−SeSx All-Solid-State Lithium Batteries. *Adv. Mater.* **2019**, *31*, 1808100.
(33) Chen, H.; Wang, C.; Dong, W.; Lu, W.; Du, Z.; Chen, L. Monodispersed sulfur nanoparticles for lithium−sulfur batteries with theoretical performance. *Nano Lett.* **2015**, *15*, 798−802.
(34) Wang, C.; Adair, K. R.; Liang, J.; Li, X.; Sun, Y.; Li, X.; Wang, J.; Sun, Q.; Zhao, F.; Lin, X.; Li, R.; Huang, H.; Zhang, L.; Yang, R.; Lu, S.; Sun, X. Solid-State Plastic Crystal Electrolytes: Effective Protection Interlayers for Sulfide-Based All-Solid-State Lithium Metal Batteries. *Adv. Funct. Mater.* **2019**, *29*, 1900392.
(35) Chen, H.; Wang, C.; Dai, Y.; Qiu, S.; Yang, J.; Lu, W.; Chen, L. Rational Design of Cathode Structure for High Rate Performance Lithium−Sulfur Batteries. *Nano Lett.* **2015**, *15*, 5443−5448.
(36) Wang, C.; Hwang, S.; Jiang, M.; Liang, J.; Sun, Y.; Adair, K.; Zheng, M.; Mukherjee, S.; Li, X.; Li, R.; Huang, H.; Zhao, S.; Zhang, L.; Lu, S.; Wang, J.; Singh, C. V.; Su, D.; Sun, X. Deciphering Interfacial Chemical and Electrochemical Reactions of Sulfide-Based All-Solid-State Batteries. *Adv. Energy Mater.* **2021**, *11*, 2100210.
(37) Wang, C.; Liang, J.; Hwang, S.; Li, X.; Zhao, Y.; Adair, K.; Zhao, C.; Li, X.; Deng, S.; Lin, X.; Yang, X.; Li, R.; Huang, H.; Zhang, L.; Lu, S.; Su, D.; Sun, X. Unveiling the critical role of interfacial ionic conductivity in all-solid-state lithium batteries. *Nano Energy* **2020**, *72*, 104686.
(38) Wang, C.; Liang, J.; Jiang, M.; Li, X.; Mukherjee, S.; Adair, K.; Zheng, M.; Zhao, Y.; Zhao, F.; Zhang, S.; Li, R.; Huang, H.; Zhao, S.; Zhang, L.; Lu, S.; Singh, C. V.; Sun, X. Interface-assisted in-situ growth of halide electrolytes eliminating interfacial challenges of all-inorganic solid-state batteries. *Nano Energy* **2020**, *76*, 105015.
(39) Wang, C.; Yu, R.; Hwang, S.; Liang, J.; Li, X.; Zhao, C.; Sun, Y.; Wang, J.; Holmes, N.; Li, R.; Huang, H.; Zhao, S.; Zhang, L.; Lu, S.; Su, D.; Sun, X. Single crystal cathodes enabling high-performance all-solid-state lithium-ion batteries. *Energy Storage Mater.* **2020**, *30*, 98−103.
(40) Deng, S.; Li, X.; Ren, Z.; Li, W.; Luo, J.; Liang, J.; Liang, J.; Banis, M. N.; Li, M.; Zhao, Y.; Li, X.; Wang, C.; Sun, Y.; Sun, Q.; Li, R.; Hu, Y.; Huang, H.; Zhang, L.; Lu, S.; Luo, J.; Sun, X. Dual-functional interfaces for highly stable Ni-rich layered cathodes in sulfide all-solid-state batteries. *Energy Storage Mater.* **2020**, *27*, 117−123.
(41) Jung, S. H.; Kim, U.-H.; Kim, J.-H.; Jun, S.; Yoon, C. S.; Jung, Y. S.; Sun, Y.-K. Ni-Rich Layered Cathode Materials with Electrochemo-Mechanically Compliant Microstructures for All-Solid-State Li Batteries. *Adv. Energy Mater.* **2020**, *10*, 1903360.
(42) Liu, X.; Zheng, B.; Zhao, J.; Zhao, W.; Liang, Z.; Su, Y.; Xie, C.; Zhou, K.; Xiang, Y.; Zhu, J.; Wang, H.; Zhong, G.; Gong, Z.; Huang, J.; Yang, Y. Electrochemo-Mechanical Effects on Structural Integrity of Ni-Rich Cathodes with Different Microstructures in All Solid-State Batteries. *Adv. Energy Mater.* **2021**, *11*, 2003583.
(43) Yan, P.; Zheng, J.; Liu, J.; Wang, B.; Cheng, X.; Zhang, Y.; Sun, X.; Wang, C.; Zhang, J.-G. Tailoring grain boundary structures and chemistry of Ni-rich layered cathodes for enhanced cycle stability of lithium-ion batteries. *Nat. Energy* **2018**, *3*, 600−605.
(44) Li, X.; Banis, M.; Lushington, A.; Yang, X.; Sun, Q.; Zhao, Y.; Liu, C.; Li, Q.; Wang, B.; Xiao, W.; Wang, C.; Li, M.; Liang, J.; Li, R.; Hu, Y.; Goncharova, L.; Zhang, H.; Sham, T.-K.; Sun, X. A high-energy sulfur cathode in carbonate electrolyte by eliminating polysulfides via solid-phase lithium-sulfur transformation. *Nat. Commun.* **2018**, *9*, 4509.
(45) Umeshbabu, E.; Zheng, B.; Yang, Y. Recent Progress in All-Solid-State Lithium−Sulfur Batteries Using High Li-Ion Conductive Solid Electrolytes. *Electrochem. Energy Rev.* **2019**, *2*, 199−230.
(46) Li, X.; Liang, J.; Banis, M. N.; Luo, J.; Wang, C.; Li, W.; Li, X.; Sun, Q.; Hu, Y.; Xiao, Q.; Sham, T.-K.; Zhang, L.; Zhao, S.; Lu, S.; Huang, H.; Li, R.; Sun, X. Totally compatible P4S10+n cathodes with self-generated Li+ pathways for sulfide-based all-solid-state batteries. *Energy Storage Mater.* **2020**, *28*, 325−333.
(47) Li, X.; Liang, J.; Li, X.; Wang, C.; Luo, J.; Li, R.; Sun, X. High-performance all-solid-state Li−Se batteries induced by sulfide electrolytes. *Energy Environ. Sci.* **2018**, *11*, 2828.
(48) Wan, H.; Mwizerwa, J. P.; Qi, X.; Liu, X.; Xu, X.; Li, H.; Hu, Y.-S.; Yao, X. Core−Shell Fe1−xS@Na2.9PS3.95Se0.05 Nanorods for Room Temperature All-Solid-State Sodium Batteries with High Energy Density. *ACS Nano* **2018**, *12*, 2809−2817.
(49) Yao, X.; Huang, N.; Han, F.; Zhang, Q.; Wan, H.; Mwizerwa, J. P.; Wang, C.; Xu, X. High-Performance All-Solid-State Lithium−Sulfur Batteries Enabled by Amorphous Sulfur-Coated Reduced Graphene Oxide Cathodes. *Adv. Energy Mater.* **2017**, *7*, 1602923.
(50) Yao, X.; Liu, D.; Wang, C.; Long, P.; Peng, G.; Hu, Y.-S.; Li, H.; Chen, L.; Xu, X. High-energy all-solid-state lithium batteries with ultralong cycle life. *Nano Lett.* **2016**, *16*, 7148−7154.
(51) Zhao, C.; Zhu, Y.; Sun, Q.; Wang, C.; Luo, J.; Lin, X.; Yang, X.; Zhao, Y.; Li, R.; Zhao, S.; Huang, H.; Zhang, L.; Lu, S.; Gu, M.; Sun, X. Transition of the Reaction from Three-Phase to Two-Phase by Using a Hybrid Conductor for High-Energy-Density High-Rate Solid-State Li-O2 Batteries. *Angew. Chem., Int. Ed.* **2021**, *60*, 5821−5826.
(52) Sun, Y.; Zhao, Y.; Wang, J.; Liang, J.; Wang, C.; Sun, Q.; Lin, X.; Adair, K. R.; Luo, J.; Wang, D.; Li, R.; Cai, M.; Sham, T.-K.; Sun, X. A Novel Organic "Polyurea" Thin Film for Ultralong-Life Lithium-Metal

Anodes via Molecular-Layer Deposition. *Adv. Mater.* **2019**, *31*, 1806541.
(53) Zhao, Y.; Amirmaleki, M.; Sun, Q.; Zhao, C.; Codirenzi, A.; Goncharova, L. V.; Wang, C.; Adair, K.; Li, X.; Yang, X.; Zhao, F.; Li, R.; Filleter, T.; Cai, M.; Sun, X. Natural SEI-Inspired Dual-Protective Layers via Atomic/Molecular Layer Deposition for Long-Life Metallic Lithium Anode. *Matter* **2019**, *1*, 1215−1231.
(54) Albertus, P.; Anandan, V.; Ban, C.; Balsara, N.; Belharouak, I.; Buettner-Garrett, J.; Chen, Z.; Daniel, C.; Doeff, M.; Dudney, N. J.; Dunn, B.; Harris, S. J.; Herle, S.; Herbert, E.; Kalnaus, S.; Libera, J. A.; Lu, D.; Martin, S.; McCloskey, B. D.; McDowell, M. T.; Meng, Y. S.; Nanda, J.; Sakamoto, J.; Self, E. C.; Tepavcevic, S.; Wachsman, E.; Wang, C.; Westover, A. S.; Xiao, J.; Yersak, T. Challenges for and Pathways toward Li-Metal-Based All-Solid-State Batteries. *ACS Energy Lett.* **2021**, 1399−1404.
(55) Wang, H.; Liu, Y.; Li, Y.; Cui, Y. Lithium Metal Anode Materials Design: Interphase and Host. *Electrochem. Energy Rev.* **2019**, *2*, 509−517.
(56) Wang, C.; Zhao, Y.; Sun, Q.; Li, X.; Liu, Y.; Liang, J.; Li, X.; Lin, X.; Li, R.; Adair, K. R.; Zhang, L.; Yang, R.; Lu, S.; Sun, X. Stabilizing interface between Li10SnP2S12 and Li metal by molecular layer deposition. *Nano Energy* **2018**, *53*, 168−174.
(57) Liang, J.; Li, X.; Zhao, Y.; Goncharova, L. V.; Wang, G.; Adair, K. R.; Wang, C.; Li, R.; Zhu, Y.; Qian, Y.; Zhang, L.; Yang, R.; Lu, S.; Sun, X. In Situ Li3PS4 Solid-State Electrolyte Protection Layers for Superior Long-Life and High-Rate Lithium-Metal Anodes. *Adv. Mater.* **2018**, *30*, 1804684.
(58) Liang, J.; Li, X.; Zhao, Y.; Goncharova, L. V.; Li, W.; Adair, K. R.; Banis, M. N.; Hu, Y.; Sham, T.-K.; Huang, H.; Zhang, L.; Zhao, S.; Lu, S.; Li, R.; Sun, X. An Air-Stable and Dendrite-Free Li Anode for Highly Stable All-Solid-State Sulfide-Based Li Batteries. *Adv. Energy Mater.* **2019**, *9*, 1902125.
(59) Zhao, F.; Sun, Q.; Yu, C.; Zhang, S.; Adair, K.; Wang, S.; Liu, Y.; Zhao, Y.; Liang, J.; Wang, C.; Li, X.; Li, X.; Xia, W.; Li, R.; Huang, H.; Zhang, L.; Zhao, S.; Lu, S.; Sun, X. Ultrastable Anode Interface Achieved by Fluorinating Electrolytes for All-Solid-State Li Metal Batteries. *ACS Energy Lett.* **2020**, *5*, 1035−1043.

https://doi.org/10.1021/accountsmr.1c00137
Acc. Mater. Res. 2022, 3, 21−32